Nitro Group as a Means of Attaching Organic Molecules to Silicon: Nitrobenzene on Si(100)-2 × 1

Lucila P. Méndez De Leo and Andrew V. Teplyakov*

Department of Chemistry and Biochemistry, University of Delaware, Newark, Delaware 19716

Received: December 20, 2005; In Final Form: February 2, 2006

This paper will present the computational and experimental infrared studies of the reactions of nitrobenzene on a Si(100) surface, a prototypical model reaction for understanding the behavior of bifunctional molecules on semiconductor surfaces. The initial reaction of nitrobenzene with the Si(100)-2 × 1 occurs via 1,3-dipolar cycloaddition of the nitro group to the silicon surface dimer. Computational exploration of the initial adsorption configurations suggests that two stable structures can be formed: one with the phenyl ring essentially perpendicular to the surface; the other one with the tilt angle of approximately 113° with respect to the surface normal. The barrier for converting the latter into the former, more stable by approximately 13 kJ/mol, is 19.1 kJ/mol. Further thermal reactions are analyzed, and the reaction pathways are compared for the computational models with fixed vs relaxed subsurface silicon atoms. While all the surface species resulting from nitrobenzene transformations on the Si(100)-2 × 1 surface studied here are thermodynamically stable, most of the reaction pathways can be ruled out on the basis of the analysis of the transition states leading to these species and on the comparison of predicted and measured vibrational spectra. As a result, the exact adsorption configurations can be pinpointed.

1. Introduction

There has been a growing interest in recent years in the combination of organic materials with conventional semiconductors.[1−4] The deposition of layers of organic molecules on a silicon surface is a way of providing a predictable and controllable functionality to the surface. This new functionality can be designed to create useful devices in microelectronics technology, catalysis, and biological sensing.

The interaction between organic molecules and semiconductor surfaces is mainly of a covalent nature. This allows for a molecular-level description of the interaction. The focus of the present study is to combine experimental and computational approaches to understand the chemistry of nitrobenzene on a Si(100)-2 × 1 surface and to explore the properties of nitro compounds relevant to silicon modification in general.

The nature of the silicon dimers on a Si(100)-2 × 1 surface suggests a unique set of chemical characteristics.[5] Certain parallels have been drawn between the chemistry of this surface and the behavior of the unsaturated organic compounds.[6−11]

The initial reaction of the nitrobenzene and the silicon surface occurs via the nitro group, as was confirmed previously.[11] This 1,3-dipolar cycloaddition process is analogous to the known reaction with unsaturated C═C bonds.[12] Nitrobenzene reactions with disilenes were also demonstrated to proceed via essentially the same pathway, as shown by Gillette et al.[13] Interestingly, the cycloaddition reaction of nitrobenzene with tertramesityldisilene was followed by the migration of one of the oxygen atoms from the nitro group into the Si−Si back-bond of the side chain.

A similar behavior was previously noted for nitromethane on Si(100)-2 × 1. The theoretical studies by Barriocanal and Doren[14,15] were based on a computational approach using density functional theory, with the B3LYP functional, and the Gaussian98 suite of programs.

Barriocanal and Doren[14] observed that the [4 + 2] pericyclic addition of nitromethane to a silicon dimer leads to the formation of a five-membered ring. The investigation of the mechanism of this addition yielded no evidence of an activation barrier. Experimental studies by Bocharov et al.[11,16] estimated an activation barrier of 36 kJ/mol for the reaction of nitromethane and nitroethane on Si(100)-2 × 1 and of 40.8 kJ/mol for nitrobenzene on Si(100)-2 × 1. The explanation for such a discrepancy was based on several factors: variety of adsorption configurations in a physisorbed monolayer as opposed to an idealized adsorption pathway used in computational studies; the role of intermolecular interactions among the adsorbed molecules; and possibly the entropy loss during the chemisorption. All of the above may contribute to the reaction barrier observed in the experimental studies. Barriocanal and Doren[14] also found that though the five-membered cycle is stable with respect to reactants (a gas-phase nitromethane molecule and a Si_9H_{12} cluster), it can give several rearrangement products involving oxygen migration into the silicon crystal. These rearrangement products are energetically favorable because of the formation of Si−O bonds at the cost of less stable N−O bonds. It was also demonstrated that structures with the maximum number of Si−O bonds are more stable. Among the structures with the same number of Si−O bonds, the less strained structures are more stable.

Eng et al.[17] used a combination of X-ray photoelectron experimental studies (XPS) and computational investigation to understand the adsorption of nitromethane on Si(100)-2 × 1. In that study, the predicted N 1s core-level shifts were used to identify the surface species. The chemical shifts corresponding to the structures with NSi_2, NOSi, and NO_2 atomic combinations were all observed in the nitrogen XPS spectrum. Despite the significant energy difference among these groups (that would

* Corresponding author. Telephone: (302) 831-1969. Fax: (302) 831-6335. E-mail: andrewt@udel.edu.

10.1021/jp057415x CCC: $33.50
Published on Web 03/16/2006

have implied that most of the products would have had to be in the most stable form: with the N bonded to two Si atoms), it was experimentally confirmed that detectable amounts of all three types of structures were present on a surface at room temperature. This finding suggests that in this case thermodynamics does not solely govern the distribution of surface products and that an important kinetic factor is present. Without a detailed investigation of the energy landscape, however, the identification of surface intermediates based on XPS spectra and computationally obtained stability of suggested surface intermediates was not possible.

In this work, we have investigated the reaction of nitrobenzene on a Si(100)-2 × 1 surface. In addition to the nitro-group reaction with the Si(100)-2 × 1 surface, the role of the phenyl group was investigated. A set of predicted surface structures was optimized without any geometrical constraints and was compared to the models with fixed positions of the subsurface atoms. The properties of a real system are thought to fall between these two limiting cases. In addition, the effect of the zero point correction energy on the predicted stability of the surface intermediates was examined.

The force constants and resulting vibrational frequencies were computed and the results compared with experimental data. To understand the experimental vibrational spectra recorded for the nitrobenzene adsorbed on a Si(100)-2 × 1 surface, the activation barriers for selected reaction pathways were calculated in an attempt to explain the coexistence of multiple surface structures similar to those observed previously for nitromethane by XPS.[17]

In addition, an interesting previously unobserved stable surface species with the resulting C−N bond (and as a consequence the phenyl ring) almost parallel to the surface is proposed.

This flexibility combined with the nature of the phenyl group provides a sensible means to study self-assembly and modification of silicon surfaces with nitro compounds.

2. Methods

2.1. Computational Methods. Electronic structure calculations were performed using the B3LYP hybrid density functional,[18,19] as implemented in the Gaussian 03 suite of programs.[20] The Si(100)-2 × 1 surface was modeled by a Si_9H_{12} cluster containing one bare single dimer and subsurface silicon atoms terminated by hydrogen to maintain their hybridization. This cluster, though, does not consider interactions with other dimers, provides predictions that are in excellent agreement with experimental results.[21−24] Some additional computational studies were performed on a two-dimer cluster model, $Si_{15}H_{16}$. In this case, the subsurface atoms representing the third layer and higher were always fixed at the positions of the fully-optimized bare two-dimer cluster to avoid nonrealistic distortions of the cluster model.

For models based on the Si_9H_{12} cluster, calculations of energy and vibrational frequencies were performed without geometrical constraints, as well as with subsurface atoms fixed. The fixed positions for the atoms representing the subsurface third layer and higher were determined from optimized structure **I** in Figure 1. In this structure, the nitrobenzene reacts only with the two top silicon atoms of the silicon structure. This is an initial structure for all further chemical rearrangements. Using structure **I** in Figure 1 to determine the coordinates for the fixed subsurface models (as opposed to using a bare silicon dimer cluster) does not have a noticeable effect on the *relative* energetics of the surface reactions studied.

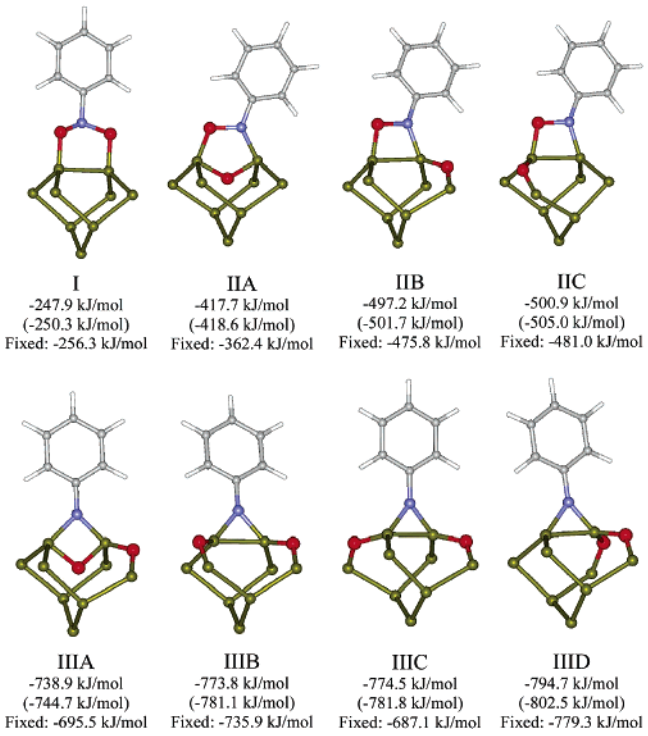

Figure 1. Optimized structures and relative energies (compared to a fully optimized nitrobenzene molecule and a Si_9H_{12} model cluster) for the different products of the reaction of nitrobenzene with the Si(100)-2 × 1 surface considered in this work. Energies listed under each structure were calculated using the B3LYP/6-311+G(d,p) level of theory. Relative energies without zero point correction are given in parentheses. Also energies calculated with fixed subsurface atoms are presented. Color scheme: green, silicon; red, oxygen; blue, nitrogen; gray, carbon; white, hydrogen. Same color-coding is used in all other figures. Hydrogen atoms terminating silicon cluster are omitted for clarity.

For this study, the geometry optimizations and reaction pathways were performed using a split valence polarized basis set with diffuse functions: 6-311+G(d,p).[25−33] When a two-dimer cluster was considered, a smaller basis set, 6-31+G(d), was used to avoid long computation times.

Vibrational frequency calculations were preformed at the same level of theory as optimization. All calculated minima for fully relaxed models were found to have no imaginary vibrational frequencies, while the transition-state structures were found to have one imaginary vibrational frequency. All calculated vibrational spectra reported were scaled to minimize the known systematic errors similarly to the approach by Bulanin et al.[34] The vibrational frequencies in these spectra were scaled by the factor 0.9564637, which is the value that provides the best fit of Si−H frequencies predicted with a single dimer cluster model to the corresponding literature experimental values for a fully occupied monohydride surface.[35−38] An additional frequency calculation with the clusters terminated with deuterium atoms was performed for each optimized model to identify the absorption peaks arising from hydrogen termination of the model cluster.

2.2. Experimental Details. The experiments were conducted in an ultrahigh-vacuum chamber located at the University of Delaware with a base pressure of 5×10^{-10} Torr. This instrument is equipped for Auger electron spectroscopy (AES), low-energy electron diffraction (LEED), and surface cleaning using an ion gun. It is also coupled to an infrared spectrometer (Nicolet, Magna 560) set up in a multiple internal reflection mode utilizing a liquid nitrogen cooled external MCT detector.

A 25 × 20 × 1 silicon Si(100)-2 × 1 trapezoidal sample with 45° beveled edges (Harrick Scientific) was used for the multiple internal reflection infrared spectroscopy studies. This sample, polished on both sides, was mounted on a manipulator capable of cooling the sample to 90 K with liquid nitrogen and heating it to above 1150 K using an e-beam heater (McAllister Technical Services).

The silicon crystals were prepared by sputtering with Ar^+ for 40 min at room temperature, followed by annealing for 20 min at 1150 K. This procedure yields a clean and well-ordered Si(100)-2 × 1 surface as confirmed by AES and LEED. Argon (Matheson, 99.999%) for surface cleaning was used without additional purification.

Nitrobenzene (99%, Aldrich) was prepurified by several freeze−pump−thaw cycles before introduction into the reaction chamber. The unshielded mass spectrometer (SRS 200) was used to determine the cleanliness of the dosing compounds in situ.

In the infrared measurements 2048 scans were collected with the resolution of 4 cm^{-1}. First the background spectrum was collected, and then the appropriate dose of the compound of interest was introduced into the ultrahigh-vacuum chamber using a leak valve. The spectrum was then collected at the same temperature as the background.

3. Results and Discussion

As indicated above, the nitro group of nitrobenzene reacts with the silicon Si(100)-2 × 1 surface by a 1,3-dipolar addition and a five-membered ring is formed. The oxygen atoms of the nitro group in nitrobenzene bind to the surface via two Si−O bonds forming an intermediate of the type presented by structure **I** in Figure 1. An asymmetric reaction path was considered to determine the activation barrier for the addition process. The product was reached by simply minimizing the energy from an initial geometry of fully optimized nitrobenzene and the silicon cluster separated by a large distance, 0.1 nm longer than a typical Si−O bond length, a value large enough to prevent significant chemical interaction. This approach was previously used by Barriocanal and Doren[14] to examine the activation barrier in reactions of nitromethane with the same cluster model. In their work both symmetric and asymmetric reaction paths were considered. In all cases, including the analysis presented here, no activation barrier was found on the basis of computational studies.

Following the same trend as that for nitromethane,[14,15] the initial surface adduct for nitrobenzene interaction with Si(100)-2 × 1 is predicted to be 247.9 kJ/mol more stable compared to reactants. This value is lower than the 300.8 kJ/mol obtained by Barriocanal and Doren[14] for nitromethane. The difference may be related to the difference in properties of substituent groups attached to the nitro group. Further studies of this factor are underway.

The possibility of a reaction of the nitro group with two adjacent surface dimers was considered. Despite the fact that the resulting surface adduct depicted in Figure 2 is not unstable, it is significantly less stable than a proposed adduct involving only one surface silicon dimer. The relative stability, as compared to the reactants, of the nitrobenzene adduct with two adjacent surface silicon dimers was found to be 154.0 kJ/mol. This value is almost 100 kJ/mol smaller than the stability of either one of the possible surface adducts involving a nitrobenzene and a single surface dimer, vide infra. Therefore, further transformations of the structure depicted in Figure 2 were not considered. Barriocanal and Doren[14] also found that the nitro compound bridging across two different dimers is less stable

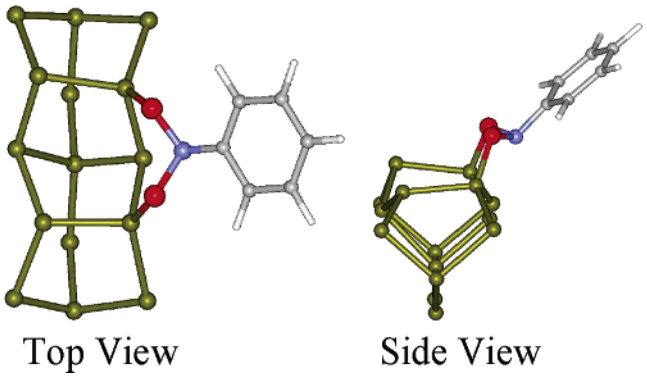

Figure 2. Alternative cycloadduct that bridges two dimers. According to computational calculations using the B3LYP/6-31+G(d) level of theory this structure is 154.0 kJ/mol more stable than isolated reactants.

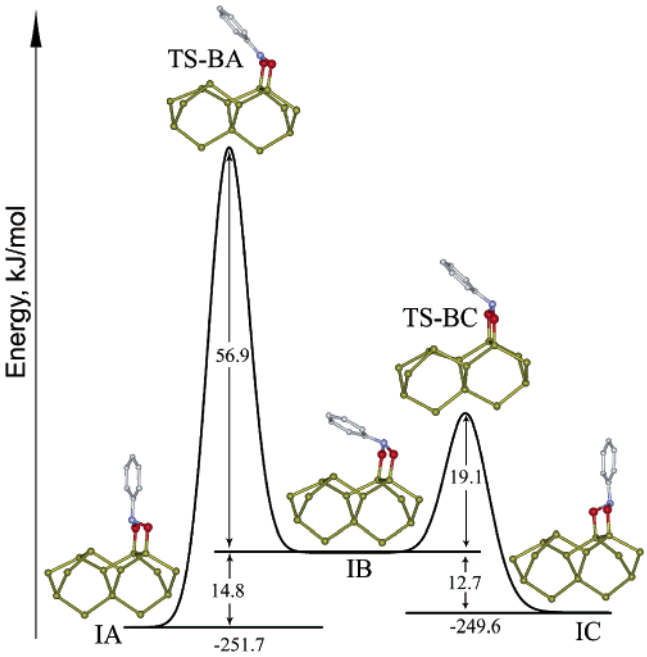

Figure 3. Proposed reaction pathway leading from structure **IB** (with the phenyl group nearly parallel to the surface) to either structure **IA** or structure **IC** with the phenyl group nearly perpendicular to the surface.

than chemisorption on a single dimer and the difference in energy was determined to be 112.1 kJ/mol, a value similar to that obtained in the present work.

Structure **I** in Figure 1 describes the result of initial interaction of nitrobenzene with the Si(100)-2 × 1 surface. However, in addition to structure **I**, there is another stable intermediate that can possibly be formed in the course of the nitrobenzene reaction with this surface. A summary of computational investigation of possible initial attachment products is outlined in Figure 3, where structures **IA** and **IC** are equivalent to structure **I**. A two-dimer model was used in these studies, and thus two possibilities for nitrobenzene bonding have to be considered: the one with the phenyl group located between the adjacent silicon dimers in the top view (structure **IA**) and the one with the phenyl group moved away from an adjacent silicon dimer (structure **IC**). On an actual silicon surface, both structures would be identical to one another. However, in a two-dimer model, they are different by 2.1 kJ/mol. Interestingly, in addition to these two stable structures, a third possibility exists for a structure with a phenyl group significantly closer to the surface, structure **IB**. This structure is only 14.8 kJ/mol less stable than structure **IA** and

12.7 kJ/mol less stable than structure **IC**. The two energy barriers presented in this figure, 56.9 and 19.1 kJ/mol, correspond to two possible rearrangement pathways. If the nitrogen atom is mainly involved in the inversion of the phenyl ring, this pathway can be described by the conversion of structure **IB** (with the phenyl group almost parallel to the silicon surface) to the structure **IA** (with the phenyl group almost perpendicular to the surface). If the rearrangement proceeds with the oxygen atoms mainly participating in this transformation, this pathway can be described as a conversion from structure **IB** to structure **IC**. In the case of the single dimer model with fixed subsurface atoms, only the pathway corresponding to the inversion of the nitrogen was calculated. A 43.6 kJ/mol barrier was found as compared to the 56.9 kJ/mol value for a two-dimer model.

These values imply that, at cryogenic temperatures, the structure with a phenyl group essentially perpendicular to the surface may coexist with the structure of the type of **IB**. However, as the temperature increases and the energy barrier is overcome, the nitrobenzene adopts the configuration with its phenyl ring perpendicular to the surface. This transformation likely involves a "flip" of the phenyl group involving the oxygen atoms and, to a lesser extent, the nitrogen atom since this second pathway is not as favorable kinetically. Thus, the structure of the type **I**, with the phenyl group almost perpendicular to the surface, was considered the starting point for all the studies presented here.

Following the formation of the initial adduct, rearrangement products involving oxygen migration into the silicon crystal can be formed. Several products can be obtained from possible rearrangements.[11,14−16] The first step would involve the migration of one of the oxygens from the five-member ring into the silicon back-bond. As illustrated in Figure 1, the structures with one oxygen inserted into a Si−Si bond are more stable than the initial adduct by approximately 250 kJ/mol, depending on the product obtained (with an exception of a less stable model **IIA**). This increase in stability seems to be due to replacing an N−O bond with a more stable Si−O bond. This step is followed by another oxygen migration into the Si−Si bond. Due to this latter migration, the resulting structures are about 270 kJ/mol more stable than the previous set (i.e. only one subsurface oxygen), the exact energy difference depending on the initial and final structures. Once again, the increase in stability seems to be due to the creation of an additional Si−O bond in place of a less stable N−O bond. As previously observed for other nitro compounds,[14] those structures that contain the maximum number of Si−O bonds and have less strained chemical bonds are more stable.

The set of data summarized in Figure 1 represents the energies computed for the fully relaxed structures with respect to the isolated reactants. The values in parentheses exclude zero point vibrational energy correction. The difference between zero point corrected relative energies and those that were not corrected is quite small (at most around 1%, for structures **IIIC** and **IIID**).

Also presented in Figure 1 are the energies of the structures obtained with fixed subsurface silicon atoms. In this latest case, no zero point vibrational energy corrections were calculated. The subsurface atoms were fixed at their positions in a fully optimized structure **I** and the energies compared with the energy of a free nitrobenzene and an unreacted Si_9H_{12} model cluster with subsurface atoms fixed at the same positions as in structure **I**. When the migration of the oxygen atoms into the silicon back-bond is considered, the fully relaxed structures are generally more stable than the fixed ones.

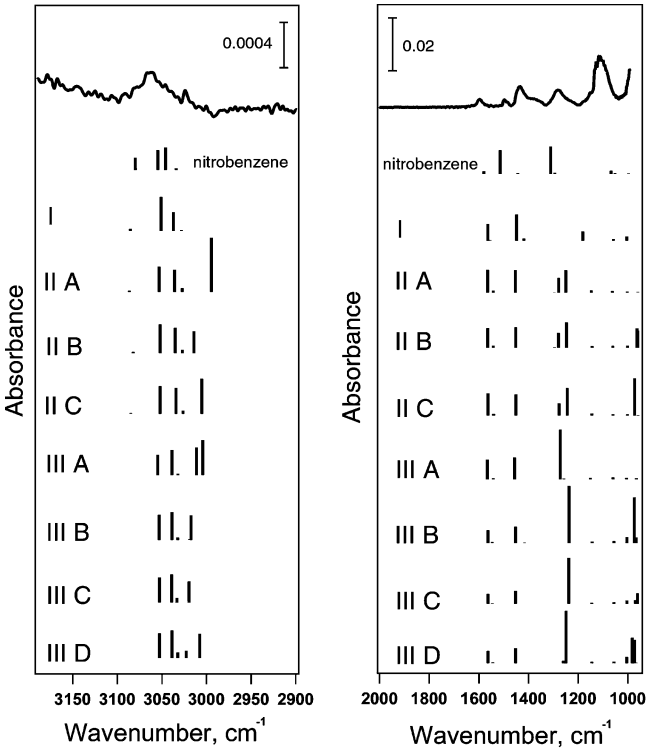

Figure 4. Comparison of experimental mid-IR FT-IR spectrum of nitrobenzene reaction on Si(100)-2 × 1 with the spectra predicted for the structures considered. A 0.9564637 scaling factor is used to account for systematic errors.

In the case of structures **IIA**, **IIB**, and **IIC**, where just one oxygen atom is moved into the silicon back-bond, the most pronounced difference between the fixed and fully relaxed structures is observed for structure **IIA**, where the oxygen atom has to insert between the Si−Si dimer atoms. This result implies that the formation of structure **IIA** is the most sensitive to the subsurface atoms being fixed.

In the case of **IIIA**, **IIIB**, **IIIC**, and **IIID** structures, both oxygen atoms are moved into the silicon back-bond. Note that the relative stability of the structures changes when the structures with fixed subsurface atoms are considered. Structure **IIIC** is the least stable if the subsurface atoms are fixed, while it is second most stable if the relaxed structure is considered. Usually when one of these structures is optimized without any positional restrictions, the silicon atoms next to the migrated oxygen tend to move outward, "opening" and thus distorting the silicon structure. In the case of structure **IIIC**, this distortion seems to be especially significant as the oxygen atoms are being inserted in the silicon back-bond at opposite sides of the dimer, affecting the whole silicon cluster. In the case of structures **IIIA** and **IIIB**, the distortion seems to be much smaller. In the case of structure **IIID**, the minimum distortion is observed, probably because only one side of the silicon dimer is altered by the oxygen migration. This analysis provides a set of computational benchmarks for understanding oxygen migration by using relaxed vs fixed subsurface models.

The trend observed for energies is in accordance with other studies of reaction of nitro compounds on a Si(100)-2 × 1 surface by means of a nitro group,[11,14,17] where migration of oxygen into the silicon crystal was observed experimentally or predicted theoretically.

Figure 4 compares the infrared spectrum obtained after a saturation exposure of nitrobenzene onto a Si(100)-2 × 1 surface at room temperature with the computationally predicted spectra

for the structures investigated. Calculations with deuterium atoms replacing the hydrogen atoms that are used to terminate model silicon clusters were also performed, and the absorption peaks around 2100 cm^{-1} were identified as arising from these Si−H vibrations. It is clear that a mixture of surface structures is obtained experimentally. However, as indicated in the left panel of Figure 4, the C−H stretch region of the spectrum, the relative intensities of the peaks around 3050 cm^{-1} of structures **IIA**, **IIC**, and **IIIA** differ drastically from the experimental spectrum. Specifically, the most prominent C−H stretch absorption bands around 3000 cm^{-1} in the computationally predicted vibrational spectra correspond to essentially zero intensity in the experiment.

These results concur with X-ray photoelectron experiments studies for adsorption of nitromethane on Si(100)-2 × 1 by Eng et al.[17] The initial adduct and different rearrangement products were considered. Among the structures considered, the possibility of migration of one or both oxygen atoms to the adjacent silicon dimer was taken into account. That possibility was not considered in the present work. However, it should be noted that according to the experimental studies of nitrobenzene,[11] the molecules of this compound react with almost every single dimer of the Si(100)-2 × 1 surface, while placing CH_3NO_2 on every dimer would result in significant steric repulsion. Thus the possibility of oxygen atoms migration to the neighboring "empty" dimer is significantly diminished on nitrobenzene-covered Si(100)-2 × 1 surfaces.

In the experimental XPS study performed by Eng et al.,[17] a N 1s spectrum was recorded after exposing a clean Si(100) surface at 223 K to 540 L of CH_3NO_2. The components of this spectrum were determined by deconvoluting it into three 80% Gaussian−20% Lorentzian curves. Three main N 1s features were found at 401.9, 400.1, and 398.5 eV. These features were assigned to molecularly adsorbed CH_3NO_2 (similar to structure **I** in Figure 1 for nitrobenzene), to rearrangement products that have just one N−O bond, and to rearrangement products where no oxygen atoms are directly attached to the nitrogen atom, respectively, on the basis of computational predictions of the N 1s core shifts. Eng et al.[17] were not able to make assignments to specific structures within each group because the differences in binding energies predicted for a set of structures within each group were much smaller than the width of the experimental features. This interpretation assigns the largest peak to the most energetically stable class of species. It is important to note that each of these groups corresponds to a class of structures considered in the present work. Molecularly adsorbed CH_3NO_2 is analogous to structure **I**; rearrangement products that have one N−O bond are analogous to structures **IIA**−**C**; and rearrangement products where no oxygen atoms are directly attached to the nitrogen atom are analogous to structures **IIIA**−**D**.

The fact that Eng et al.[17] found that the three groups of structures were present in the final product despite the significant energy difference among them (that implies only the most stable class of structures should be present) confirms that thermodynamics does not solely govern this reaction, but an important kinetic factor is present.

To explain this fact, selected reaction paths leading to different products were explored.

As mentioned above, Barriocanal and Doren have used a theoretical description to analyze in detail the first step of nitro-group-containing compounds with a Si(100)-2 × 1 surface.[14] Regardless of the exact mechanism of this reaction, the barrier for this transformation was determined to be negligibly small.

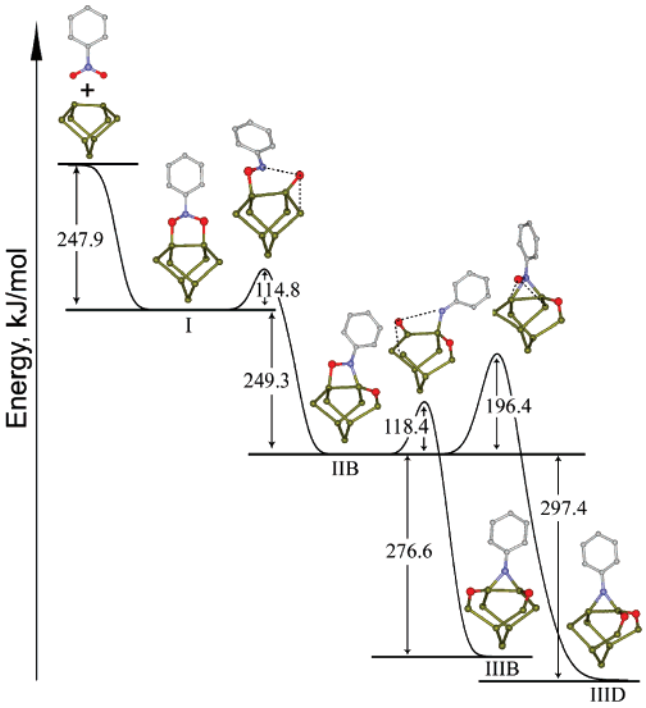

Figure 5. Reaction pathways for some of the processes of oxygen insertion into the Si−Si bonds. Values were obtained using the fully relaxed model for the silicon cluster.

The activation barriers for further surface reactions of the nitro group were not analyzed previously. In this manuscript, a detailed investigation of further surface processes involving the migration of oxygen atoms into silicon back-bonds is presented. This analysis assumes that only one oxygen atom can change its position at a time. Starting with structure **I**, the possibilities of forming essentially any surface species consistent with the experimental infrared spectrum collected at room temperature are summarized in Figure 5 for the fully relaxed cluster model and Figure 6 for the computational investigation of a Si_9H_{12} cluster with the positions of the subsurface atoms fixed at the same coordinates as those in structure **I**.

The reaction path from structure **I** to structure **IIA** was also investigated. When the subsurface atoms were fixed (the scenario most likely to be closer to the real experimental conditions), a preliminary set of studies estimated that the barrier for the oxygen insertion between the two silicon atoms forming the dimer was 44.37 kJ/mol. This value is smaller than that for other possible reaction paths. However, according to the IR spectrum, this structure is not present in the final product mixture. Further computational studies involving the presence of several silicon dimers should be conducted to explain the absence of this structure in the final product but will not be the focus of the present work.

In the case of the reaction path from structure **I** to **IIB,** both the fully relaxed model and the fixed subsurface model were considered. The activation barrier found for this process was 114.8 kJ/mol in the case of the fully relaxed structures and 126.0 kJ/mol in the case of the fixed subsurface structures. These barriers are very similar to one another. Additionally, the structures of the transition states are similar (differences below 3% were found in distances and angles among atoms involved in the process).

The following step, involving the migration of the second oxygen to the silicon subsurface, is also presented in Figures 5 and 6. Two different possibilities were taken into account: the reactions from structure **IIB** to **IIIB** and to **IIID**. The activation

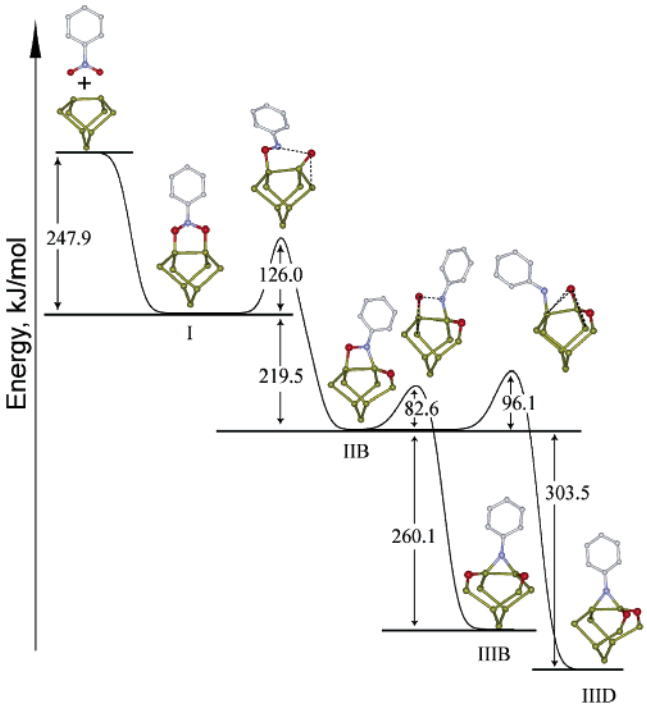

Figure 6. Reaction pathways for some of the processes of oxygen insertion into the Si−Si bonds. Values were obtained using the fixed subsurface model cluster.

barrier leading to the formation of structure **IIIB** was determined to be 118.4 kJ/mol in the case of fully relaxed structures. In the case of the subsurface fixed atoms model, the activation barrier was more difficult to find. Apparently, the migration of the oxygen is coupled with the rotation of the phenyl ring, making it difficult to predict the structure of the transition states. A value of 82.6 kJ/mol was found for a process that involves the insertion of the oxygen atom into the silicon back-bond accompanied by the phenyl group rotation. This value was considered to be a maximum limit in the activation energy for this process.

The energy barrier from structure **IIB** to **IIID** was also estimated. It was found that, in the case of fully relaxed structures, this barrier is more than twice as large as when the fixed subsurface model is considered (196.4 kJ/mol vs 96.1 kJ/mol). The reason for this difference may be related to a very significant change in the position of subsurface silicon atoms in the relaxed structure that has to be performed to accommodate the oxygen in its final position, while the positions of the atoms in a model with fixed subsurface are closer to the final state. For this reason, the structures of the transition states calculated, and subsequently the specific reaction pathways, are so different for this analysis depending on the model used (Figures 5 and 6).

Comparing the calculated energy barriers for the two possible oxygen migration pathways, we found a higher activation barrier for the latter pathway (i.e. **IIB** to **IIID**). The reason for this difference in the activation barrier is likely due to the fact that, in the second case, the oxygen atom has to migrate across the whole structure, changing its position with respect to the phenyl ring, while in the first case it does not. As a result, the oxygen atom has to be repositioned by a significantly longer distance to transform the reactant into the product. This fact implies that structure **IIID** is not a major contributor to the final product distribution, even though it is the most thermodynamically stable structure of all the models analyzed here.

Another feature to take into account is that, in the case of the fully relaxed model, the activation energy for the reaction from structure **I** to structure **IIB** and that for the reaction of structure **IIB** to form **IIIB** seem to be comparable. Furthermore, the positions of the oxygen atom moving into the Si−Si bond involved in this transformation are similar in both transition states. The distance from the oxygen atom to the closest superficial silicon atom is 0.158 and 0.159 nm for the transition state from structure **I** to structure **IIB** and from structure **IIB** to **IIIB**, respectively. The distances from the oxygen atom to the other superficial silicon atom also differ by only 0.001 nm between these structures, while the angles between the oxygen atom involved in the process and the superficial silicon dimer only differ by 2°. This similarity implies that the process of migration of each oxygen atom would not depend, to any significant extent, on the position of the other oxygen atom, so that oxygen atoms migrate largely independently. This means that the activation barrier for the reaction from structure **IIB** to **IIIC** is probably around 120 kJ/mol, as this process should be similar to the transition from structures **I** to **IIB** or from **IIB** to **IIIB**. Since structure **IIIB** is approximately 50 kJ/mol more stable than structure **IIIC** (according to the fixed subsurface atoms model), it is likely that most of the product with two oxygen atoms subsurface (i.e. structures **IIIA**−**D**) is in the form of structure **IIIB**.

In summary, structures **IIA** and **IIIA** are not present in the final product according to the comparison of the experimental IR spectrum and the predicted ones obtained by calculations. At the same time, structures **IIC** and **IIID**, though energetically accessible, may be present only in small amounts in the final mixture because the energy barrier that has to be overcome is higher than the corresponding barrier leading to other alternative thermodynamically accessible structures. Finally, structure **IIIC** has lower stability when compared to other structures equally accessible in terms of the reaction pathways and thus is suggested to only be a minor component represented in the distribution of the final products.

Since the formation of all the structures considered in this paper proceeds downhill, compared to the unreacted nitrobenzene and clean silicon surface, the initial absorption energy could be sufficient to overcome all the interstructural barriers to form the most thermodynamically stable structures. However, some of this energy maybe lost upon the adsorption process, for example, through surface vibrational energy modes. The exact quantitative description of the product distribution may aid in assessing the portion of the energy lost during adsorption.

The previous discussion indicates that although a mixture of structures is expected to be obtained as a final product,[11,17] on the basis of a comparison of the experimental and computational investigation, it is possible to narrow down the list to three major structures: **I**, **IIB**, and **IIIB**, each one having the nitrogen atom bonded to different numbers of oxygen atoms (i.e.: C and two O for structure **I**; C, Si, and O for structure **IIB**, and C and two Si for structure **IIIB**). The comparison of the experimental spectra shown in Figure 4 with the vibrational spectra predicted for these three model structures suggests that in the product mixture observed after dosing nitrobenzene at room temperature all three structures may coexist. While the infrared spectra for structures **IIB** and **IIIB** cannot be distinguished by comparison with the experimental spectra obtained within the spectral range and within the signal-to-noise ratio afforded by our experimental setup, it is most definitely that one of these structures dominates the mixture. Additional spectroscopic information will be needed for more quantitative assignment. One of the most useful

spectroscopic techniques in the future experimental investigation of this system may be XPS. XPS studies of gaseous nitrobenzene indicate that the binding energy of nitrogen N 1s in this compound is similar to the binding energy of nitrogen N 1s in nitromethane.[39] Therefore the core shifts will not be affected significantly by the nature of the carbon atom bonded to the nitrogen and the XPS spectrum will allow for the differentiation of the peaks corresponding to structures **I**, **IIB**, and **IIIB**, thus providing the possibility to quantify the structures present in the final product distribution.

4. Conclusions

The computational studies performed of the reaction of nitrobenzene on Si(100)-2 × 1 led to a better understanding of this reaction. Two types of models were considered: fully relaxed silicon cluster and a cluster where the subsurface atoms were fixed. These two models yielded the lower and upper limits for the energy of the structures studied. The zero point correction was considered for the relaxed model and found to have a negligible effect on the relative stability of surface species in all cases analyzed.

A structure of the first cycloadduct (before migration of oxygen into the silicon crystal) with the benzene ring almost parallel to the silicon surface was found to be a local minimum in energy. Optimization of this structure on a two-dimer cluster was performed, and the reaction path from this structure to the more stable structure, with the phenyl ring perpendicular to the silicon surface, was also analyzed. A significant activation barrier was found, which indicates that at low temperatures both structures may be present, but as temperature increases only the most stable structure will prevail.

On the basis of a combination of infrared spectroscopic studies and computational analysis of possible reaction pathways, structures **IIA**, **IIC**, and **IIIA** could be ruled out as major products of the reaction of nitrobenzene with the silicon surface. Moreover, on the basis of thermodynamics and kinetics considerations, it can be concluded that structures **IIIC** and **IIID** are also not major contributors to the final product distribution.

These results indicate that kinetics plays an important role in the selection of the final structures present. The products that can be formed on a Si(100)-2 × 1 surface via pathways with lower activation energy have a higher probability to be present in the final product distribution than those with higher activation barriers (**IIB** to **IIIB** vs **IIB** to **IIID**).

It was possible to obtain a complete picture of the processes taking place during the reaction of nitrobenzene with a Si(100)-2 × 1 surface. From the comparison of the experimental IR spectrum of the reaction of nitrobenzene on a Si(100)-2 × 1 surface with the computationally predicted vibrational frequencies for the different possible surface structures, and considering the relative stability and activation barriers required to reach these structures, structures **I**, **IIB**, and **IIIB** are present as a result of nitrobenzene reaction with the Si(100)-2 × 1 surface. Reaction-specific quantitative information can be further obtained by XPS studies.

Acknowledgment. Acknowledgment is made to the National Science Foundation (Grant CHE-0313803) for the support of this research. A.V.T. also thanks Professor Douglas J. Doren, Mr. Jeffrey Frey, and Dr. Olga Dmitrenko (Department of Chemistry and Biochemistry, University of Delaware) for useful discussions.

Supporting Information Available: Cartesian coordinates and IR frequencies and complete ref 20 (pdf). This material is available free of charge via the Internet at http://pubs.acs.org.

References and Notes

(1) Bent, S. F. *Surf. Sci.* **2002**, *500*, 879.
(2) Buriak, J. M. *Chem. Rev.* **2002**, *102*, 1272.
(3) Wolkow, R. A. *Annu. Rev. Phys. Chem.* **1999**, *50*, 413.
(4) Bent, S. F. *J. Phys. Chem. B* **2002**, *106*, 2830.
(5) Chadi, D. J. *Phys. Rev. Lett.* **1979**, *43*, 43.
(6) Teplyakov, A. V.; Kong, M. J.; Bent, S. F. *J. Chem. Phys.* **1998**, *108*, 4599.
(7) Kong, M. J.; Teplyakov, A. V.; Lyubovitski, J. G.; Bent, S. F. *Surf. Sci.* **1998**, *411*, 286.
(8) Konecny, R.; Doren, D. J. *Surf. Sci.* **1998**, *417*, 169.
(9) Choi, H. C.; Gordon, M. S. *J. Am. Chem. Soc.* **1999**, *121*, 11311.
(10) Clemen, L.; Wallace, R. M.; Taylor, P. A.; Dresser, M. J.; Choyke, W. J.; Weinberg, W. H.; Yates, J. T. J. *Surf. Sci.* **1992**, *268*, 205.
(11) Bocharov, S.; Teplyakov, A. V. *Surf. Sci.* **2004**, *573*, 403.
(12) Padwa, A. *1,3-Dipolar cycloaddition chemistry*; Wiley-Interscience: New York, 1984.
(13) Gillette, G. R.; Maxka, J.; West, R. *Angew. Chem., Int. Ed. Engl.* **1989**, *28*, 54.
(14) Barriocanal, J. A.; and Doren, D. J. *J. Phys. Chem. B* **2000**, *104*, 12269.
(15) Barriocanal, J. A.; Doren, D. J. *J. Vac. Sci. Technol., A* **2000**, *18*, 1959.
(16) Bocharov, S.; Mathauser, A. T.; Teplyakov, A. V. *J. Phys. Chem. B* **2003**.
(17) Eng, J.; Hubner, I. A.; Barriocanal, J.; Opila, R. L.; Doren, D. J. *J. Appl. Phys.* **2004**, *95*, 1963.
(18) Becke, A. D. *J. Chem. Phys.* **1993**, *98*, 1372.
(19) Lee, C.; Yang, W.; Parr, R. G. *Phys. Rev. B* **1988**, *37*, 785.
(20) Frisch, M. J. T.; et al. *Gaussian 03*, Revision C.02; Gaussian, Inc.: Wallingford CT, 2004.
(21) Nachtigall, P.; Jordon, K. D.; Janda, K. C. *J. Chem. Phys.* **1991**, *95*, 8652.
(22) Konecny, R.; Doren, D. J. *J. Chem. Phys.* **1997**, *106*, 2426.
(23) Widjaja, Y.; Mysinger, M. M.; Musgrave, C. B. *J. Phys. Chem. B* **2000**, *104*, 2527.
(24) Mui, C.; Wang, G. T.; Bent, S. F.; Musgrave, C. B. *J. Chem. Phys.* **2001**, *114*, 10170.
(25) McLean, A. D.; Chandler, G. S. *J. Chem. Phys.* **1980**, *72*, 5639.
(26) Krishnan, R.; Binkley, J. S.; Seeger, R.; Pople, J. A. *J. Chem. Phys.* **1980**, *72*, 650.
(27) Blandeau, J. P.; McGrath, M. P.; Cusrtiss, L. A.; Radom, L. *J. Chem. Phys.* **1997**, *107*, 5016.
(28) Wachters, A. J. H. *J. Chem. Phys.* **1970**, *52*, 1033.
(29) Hay, P. J. *J. Chem. Phys.* **1977**, *91*, 1206.
(30) Raghavachari, K.; Trucks, G. W. *J. Chem. Phys.* **1989**, *91*, 1206.
(31) Binning, R. C., Jr.; Curtiss, L. A. *J. Comput. Chem.* **1995**, *11*, 1206.
(32) Curtiss, L. A.; McGrath, M. P.; Blandeau, J. P.; Davis, N. E.; Binning, R. C., Jr.; Radom, L. *J.* Chem. Phys. **1995**, *103*, 9104.
(33) McGrath, M. P.; Radom, L. *J. Chem. Phys.* **1991**, *94*, 511.
(34) Bulanin, K. M.; Shah, A. G.; Fitzgerald, D. R.; Doren, D. J.; Teplyakov, A. V. *J. Phys. Chem. B* **2002**, *106*, 7286.
(35) Chabal, Y. J.; Raghavachari, K. *Phys. Rev. Lett.* **1984**, *53*, 282.
(36) Chabal, Y. J. *Surf. Sci.* **1986**, *168*, 594.
(37) Chabal, Y. J. *Surf. Sci. Rep.* **1988**, 211.
(38) Chabal, Y. J. *Physica B* **1991**, *170*, 447.
(39) Jolly, W. L.; Bombem, K. D.; Eyermann, C. J. *At. Data Nucl. Data Tables* **1984**, *31*, 433.